

# Electrochemical immobilization of Cs in single-crystalline SYNROC

Hideki Abe\*, Akira Satoh, Kenji Nishida, Eiji Abe, Takashi Naka,  
Motoharu Imai, Hideaki Kitazawa

National Institute for Materials Science (NIMS), Sengen 1-2-1, Tsukuba, Ibaraki 305-0047, Japan

Received 18 December 2005; received in revised form 31 January 2006; accepted 4 February 2006  
Available online 10 March 2006

## Abstract

The development of a disposal technique for the radiotoxic  $^{137}\text{Cs}$  in nuclear wastes is one of the most urgent issues in nuclear fuel technology. An effective disposal method of  $^{137}\text{Cs}$  is to immobilize it in a synthetic rock (SYNROC) material: cesium titanate hollandite,  $^{137}\text{Cs}_x\text{Ti}_8\text{O}_{16}$  ( $I4/m$ ,  $a = 10.2866(3)\text{Å}$ ,  $c = 2.9669(1)\text{Å}$ ). Practical applications of  $^{137}\text{Cs}_x\text{Ti}_8\text{O}_{16}$  have been restricted so far because the conventional synthetic method requires strong chemical reducers and reaction temperatures higher than  $1250^\circ\text{C}$ . In this report, we present a milder preparation method of  $\text{Cs}_x\text{Ti}_8\text{O}_{16}$  by electrolysis of a mixture of  $\text{Cs}_2\text{MoO}_4$  and  $\text{TiO}_2$  in ambient atmosphere at  $900^\circ\text{C}$ . The Cs content in the resultant *single-crystalline*  $\text{Cs}_{1.35}\text{Ti}_8\text{O}_{16}$  is competitive with the highest value in polycrystalline  $\text{Cs}_{1.36\pm 0.03}\text{Ti}_8\text{O}_{16}$  prepared by the conventional synthetic method. The electrochemical preparation of  $\text{Cs}_{1.35}\text{Ti}_8\text{O}_{16}$  is a promising way to immobilize a high quantity of  $^{137}\text{Cs}$  ions in a stable form of single-crystalline SYNROC.

© 2006 Elsevier Inc. All rights reserved.

**Keywords:**  $^{137}\text{Cs}$ ; Nuclear wastes; Immobilization; SYNROC; Cesium titanate hollandite;  $^{137}\text{Cs}_x\text{Ti}_8\text{O}_{16}$ ; Electrochemical preparation; Single crystals

## 1. Introduction

The development of a disposal technique for high concentrations of the radioactive  $^{137}\text{Cs}$  contained in nuclear wastes is one of the most urgent issues in the field of nuclear fuel technology for two reasons. First, radioactive  $^{137}\text{Cs}$  is highly toxic compared to the other radioactive elements because the half lifetime of  $^{137}\text{Cs}$  is close to the average life spans of higher living organisms [1]. Secondly, the ionized  $^{137}\text{Cs}$  disperses widely into the environment because of its high solubility in water.

An effective disposal method of the radioactive  $^{137}\text{Cs}$  is to make it water insoluble by fixing it in solid matrix materials called synthetic rocks (SYNROC) and then to bury them deeply in the ground [2–5]. A SYNROC material is required not only to contain as much  $^{137}\text{Cs}$  as possible but also to possess sufficient leach resistance for a long period of time.

The cesium titanate hollandite,  $\text{Cs}_x\text{Ti}_8\text{O}_{16}$  ( $x = 1.06–1.36 \pm 0.03$ ), was proposed as a promising SYNROC

material for the disposal of radioactive  $^{137}\text{Cs}$  because Cs ions are encapsulated stably within the one-dimensional oxygen cavities formed by ledge-sharing of the  $\text{TiO}_6$  octahedra (Fig. 1) [2–5]. Two methods for the preparation of  $\text{Cs}_x\text{Ti}_8\text{O}_{16}$  have been developed. The first is a direct reaction between elemental Cs or Cs compounds and solid-state  $\text{TiO}_2$  under reducing conditions at temperatures above  $1250^\circ\text{C}$  [6–9]. In such cases, the Cs content in the obtained  $\text{Cs}_x\text{Ti}_8\text{O}_{16}$ ,  $x = 1.33–1.36 \pm 0.03$ , was the highest value among the reported data. The second is the electrochemical reduction of a molten mixture of  $\text{TiO}_2$  and  $\text{Cs}_2\text{Ti}_2\text{O}_5$ , where  $\text{Cs}_2\text{Ti}_2\text{O}_5$  plays a role of flux to enable the formation of single-crystalline  $\text{Cs}_{1.06}\text{Ti}_8\text{O}_{16}$  at around  $1000^\circ\text{C}$  [10,11]. The low reaction temperature is preferable from the viewpoint of processing costs, however, the second method is not applicable to the immobilization of  $^{137}\text{Cs}$  in nuclear wastes because the  $\text{Cs}_2\text{Ti}_2\text{O}_5$  flux itself contains a considerable amount of Cs. In this paper, we report that single-crystalline  $\text{Cs}_x\text{Ti}_8\text{O}_{16}$  containing a high content of Cs,  $x = 1.35$ , was successfully synthesized at a lower reaction temperature of  $900^\circ\text{C}$  by electrolysis of a mixture of  $\text{Cs}_2\text{O}$ ,  $\text{MoO}_3$ , and  $\text{TiO}_2$ .

\*Corresponding author. Fax: +81 298 59 2801.

E-mail address: [ABE.Hideki@nims.go.jp](mailto:ABE.Hideki@nims.go.jp) (H. Abe).

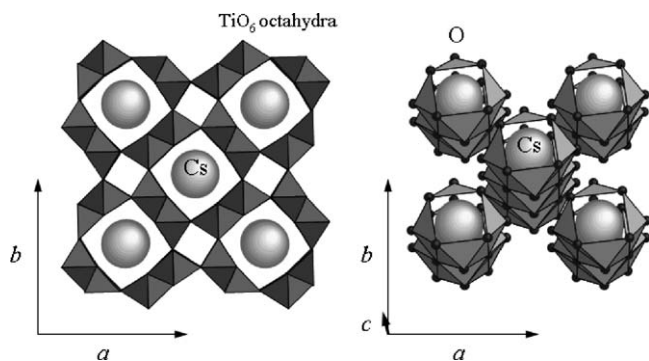


Fig. 1. Crystal structure of cesium titanate hollandite,  $\text{Cs}_x\text{Ti}_8\text{O}_{16}$ . The left and right figures show a (001) view of the crystal structure and the oxygen cavities encapsulating Cs ions, respectively.

## 2. Experimental section

An alumina boat with a size of  $10 \times 10 \times 100 \text{ mm}^3$  served as the electrolysis cell. Two Pt wires were fixed at both ends of the electrolysis cell as the working and counter electrodes. The Pt reference electrode was placed in the vicinity of the working electrode. All the electrodes were connected to Pt leads. The Cs source,  $\text{Cs}_2\text{CO}_3$  (99.99% purity, Furuuchi Chemicals Co. Ltd.), was mixed with the flux material,  $\text{MoO}_3$  (99.99% purity, Furuuchi Chemicals Co. Ltd.), in the same molar ratio and sintered to form  $\text{Cs}_2\text{MoO}_4$  at  $600^\circ\text{C}$  in ambient atmosphere. The electrolysis cell was filled with 4.0 g of powdered  $\text{Cs}_2\text{MoO}_4$ . Anatase-type  $\text{TiO}_2$  (99.98% purity, Soekawa Chemicals Co. Ltd.) powder (0.1 g) was placed on the  $\text{Cs}_2\text{MoO}_4$  powder in the vicinity of the working and reference electrodes. The electrolysis cell was then introduced into a tubular furnace that allowed the Pt leads to reach a DC power supply outside. The  $\text{TiO}_2$  and  $\text{Cs}_2\text{MoO}_4$  powders were molten at  $900^\circ\text{C}$  and in ambient atmosphere. Electrolysis for 1 h resulted in crystalline precipitates on the working electrode.

Compositional analysis was performed by electron probe microanalysis (EPMA: JEOL SM-09010) on two crystalline precipitates at different regions of each crystal. Structural characterization was performed by powder X-ray diffraction (pXRD: RIGAKU RINT 2000) measurements on the powdered crystals with  $\text{Cu-K}\alpha$  radiation ( $\lambda = 1.541 \text{ \AA}$ ) at room temperature. A crystal with dimensions of  $0.04 \times 0.04 \times 0.2 \text{ mm}^3$  was selected for the data collection of four-circle XRD. The intensities of 4921 reflections were collected by the  $\omega$ -scan method in the  $2\theta$  range from 0 to  $105^\circ$  on a Bruker SMART APEX CCD area-detector diffractometer with graphite-monochromatized  $\text{Mo-K}\alpha$  radiation ( $\lambda = 0.71073 \text{ \AA}$ ) at room temperature.

## 3. Results and discussion

Fig. 2 shows a potentiometric profile obtained in a molten  $\text{MoO}_3$  flux dissolving Cs and Ti ions at  $900^\circ\text{C}$  in

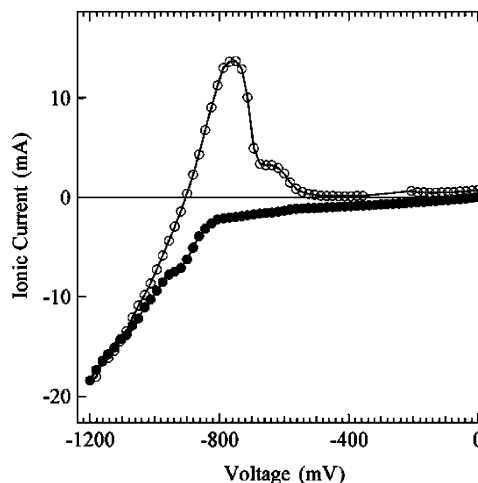


Fig. 2. Voltammetric profile in a molten  $\text{MoO}_3$  flux containing Cs and Ti ions.



Fig. 3. Optical microscope image of crystals grown at the tip of the working electrode.

ambient atmosphere. The ionic current ( $I_i$ ) from the working to the counter electrodes is plotted against the voltage applied to the working electrode ( $V_w$ ). With decreasing  $V_w$  from 0,  $I_i$  shows a drop at a critical voltage ( $V_c$ ) of  $-820 \text{ mV}$  and continues to decrease to  $-1200 \text{ mV}$  via a small hump at around  $-940 \text{ mV}$  (denoted by closed circles). When  $V_w$  increases to more than  $-1200 \text{ mV}$ ,  $I_i$  increases to overshoot across the zero axis at  $-900 \text{ mV}$  and converges on  $0 \text{ mA}$  at  $0 \text{ mV}$  via a maximum at  $-750 \text{ mV}$ . The rise in the amplitude of  $I_i$  in the decreasing profile of  $V_w$  at  $V_c$  (closed circles) suggests the formation of precipitates at  $V_w < V_c$ . The wide hysteresis in the region of  $-1000 < V_w < -500 \text{ mV}$  is attributed to the dissolution of the precipitates in the molten flux (open circles). Electrolysis in the molten flux was carried out for 1 h by

setting  $I_i$  to be a constant value of  $-10$  mA, where  $V_w$  was kept lower than  $V_c$ . Blue–black needle-shaped crystals with a length of several millimeters grew thickly on the tip of the working electrode, whereas no precipitates were recognized either on the counter or on the reference electrodes (Fig. 3).

The chemical composition was roughly evaluated by EPMA to be  $\text{Cs}_{2.0}\text{Ti}_{8.0}\text{O}_{17}$  regardless of the sampling regions, which indicates that the crystals are homogenous without micro-domains of different stoichiometry. Fig. 4 shows the result of structural analysis by pXRD on the powdered crystals. All the peaks in the pXRD profile are indexed by a tetragonal unit cell with the lattice parameters of  $a = 2.97$  and  $c = 10.3$  Å. The compositional and structural data of the crystals coincide with those of the hollandite-type titanate,  $A_x\text{Ti}_8\text{O}_{16}$  ( $A =$  alkali or alkali earth elements), which possesses a tetragonal  $I4/m$  structure with the lattice parameters of  $a \sim 3$  and  $c \sim 10$  Å. The structure was refined based on the four-circle XRD data assuming the atomic positions reported in the neutron diffraction data on polycrystalline  $\text{Cs}_{1.36 \pm 0.03}\text{Ti}_8\text{O}_{16}$  using

the SHELXL97 program (Table 1) [9]. The final refinement converged to  $wR(F_o^2) = 0.0961$  on all data and, for the 877 reflections possessing  $F^2 > 2\sigma(F^2)$ , to the conventional reliability factor  $R(F_o) = 0.0413$ . The final values of the positional parameters, isotropic equivalent atomic displacement parameters, and their standard uncertainties are listed in Table 2 together with those obtained by neutron diffraction on polycrystalline  $\text{Cs}_{1.36 \pm 0.03}\text{Ti}_8\text{O}_{16}$  (indicated in parentheses) [9]. The chemical composition of the crystals was refined to be  $\text{Cs}_{1.35}\text{Ti}_8\text{O}_{16}$  from the site occupancies of the constituent chemical species (Table 2).

The electrochemical preparation method of  $\text{Cs}_{1.35}\text{Ti}_8\text{O}_{16}$  in molten  $\text{MoO}_3$  flux possesses practical advantages over the conventional ones. First, the preparation condition at  $900$  °C and ambient atmosphere is moderate compared to the conventional direct preparation using  $\text{TiO}_2$  and Cs compounds as starting materials, which requires reaction temperatures higher than  $1250$  °C and chemical reducers, such as  $\text{H}_2$  gas or Cs metal. The harsh reaction condition of the conventional method was necessary because one of the starting materials, solid-state  $\text{TiO}_2$ , takes the highly inactive form of rutile at temperatures higher than  $1000$  °C [12]. The  $\text{MoO}_3$  flux enables the moderate formation condition of single-crystalline  $\text{Cs}_{1.35}\text{Ti}_8\text{O}_{16}$  by decomposing the solid-state  $\text{TiO}_2$  into active Ti ions in melt. The  $\text{MoO}_3$  flux also suppresses volatilization of Cs during electrolysis through formation of a  $\text{Cs}_2\text{MoO}_4$  melt. The  $\text{Cs}_2\text{MoO}_4$  melt is so thermally stable at high temperatures above  $1000$  °C in air

Table 1  
Crystallographic data and structure refinement for the single-crystalline  $\text{Cs}_{1.35}\text{Ti}_8\text{O}_{16}$

Formula	$\text{Cs}_{1.35}\text{Ti}_8\text{O}_{16}$
Molecular weight	818.606
Space group	$I4/m$
$a$ (Å)	10.2866(3)
$c$ (Å)	2.9669(1)
$V$ (Å <sup>3</sup> )	313.9(2)
$Z$	1
Density (calcd, g cm <sup>-3</sup> )	4.331
Temperature (K)	293
Diffractometer	Bruker SMART APEX CCD area-detector diffractometer
Crystal color	Blue black
Morphology	Thin plate
Crystal sizes (mm <sup>3</sup> )	$0.04 \times 0.04 \times 0.2$
Linear absorption coeff. (mm <sup>-1</sup> )	8.705
Monochromator	Graphite
Scan mode	$\omega$
Recording range $2\theta$	0–105
$hkl$ range	$-22 < h < 14; -22 < k < 21;$ $-6 < l < 6$
No. of measured reflections	4921
No. of independent reflection	996
No. of observed reflections with $F^2 > 2\sigma(F^2)$	877
$R_{\text{int}}$	0.0402
Absorption correction method	Empirical
Transmission factors (min.–max.)	0.4037–0.6559
Refinement	$F^2$
Calculated weights	$w = 1/[\sigma^2 F_o^2 + (0.0422P)^2 + 0.75P]$ where $P = (\max[F_o^2, 0] + 2F_c^2)/3$
Extinction coefficient (SHELXL 97)	0.003469
$R [F_o > 4\sigma(F_o)]$	0.0413
$R (F_o \text{ all data})$	0.0481
$wR (F_o^2) \text{ on all data}$	0.0961
Goodness-of-fit, $S$ (all data)	1.145
No. of refined parameters	24
Residual peaks (e/Å <sup>3</sup> )	$-1.19, 1.37$

Table 2  
Positional parameters and equivalent isotropic displacement parameters for the single-crystalline  $\text{Cs}_{1.35}\text{Ti}_8\text{O}_{16}$

Atom	$x$	$y$	$z$	$U_{\text{eq}}$ (Å <sup>2</sup> )	SOF
Cs	0.00000	0.00000	0.6238(3) 0.627(3) <sup>a</sup>	0.0180(2)	0.0841(4)
Ti	0.16487(3) 0.1652(3) <sup>a</sup>	0.34837(3) 0.3485(2) <sup>a</sup>	0.00000	0.0076(1)	0.50000
O1	0.2088(1) 0.2084(1) <sup>a</sup>	0.1580(1) 0.1580(2) <sup>a</sup>	0.00000	0.0066(2)	0.50000
O2	0.1671(1) 0.1664(2) <sup>a</sup>	0.5379(1) 0.5377(1) <sup>a</sup>	0.00000	0.0077(2)	0.50000

<sup>a</sup>Ref. [9].

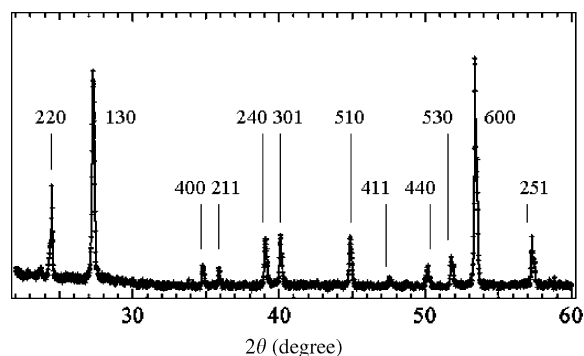


Fig. 4. Powder XRD profile of the crystals.

that it has been used as an effective flux for single-crystal growth of oxides with high melting points such as  $\text{Cr}_2\text{O}_3$  or  $\text{La}_{1-x}\text{Sr}_x\text{MnO}_3$  [13–16]. Secondly, the surface area per volume (SA/V) of the resultant single-crystalline  $\text{Cs}_{1.35}\text{Ti}_8\text{O}_{16}$  is lower than that of the polycrystalline  $\text{Cs}_{1.36\pm 0.03}\text{Ti}_8\text{O}_{16}$  obtained by the conventional method. The SA/V of single-crystalline  $\text{Cs}_{1.35}\text{Ti}_8\text{O}_{16}$ , with an averaged dimension of  $0.02 \times 0.02 \times 2 \text{ mm}^3$ , is 30 times lower than that of polycrystalline  $\text{Cs}_{1.36\pm 0.03}\text{Ti}_8\text{O}_{16}$ , with a grain size in the order of  $1 \mu\text{m}^3$ . It is strongly suggested that single-crystalline  $\text{Cs}_{1.35}\text{Ti}_8\text{O}_{16}$  is a much less leachable SYNROC material than polycrystalline  $\text{Cs}_{1.36\pm 0.03}\text{Ti}_8\text{O}_{16}$  because the leach rate of  $^{137}\text{Cs}$  is proportional to the SA/V of SYNROC [5].

The electrochemical immobilization of Cs is still on the way to the practical application because it needs pretreatments to separate  $^{137}\text{Cs}$  from the other radioactive elements contained in actual nuclear wastes. At the current moment, separation of  $^{137}\text{Cs}$  from the other radioactive elements using ion-selective materials such as silicotitanates is thought to be an effective pretreatment for the electrochemical immobilization of  $^{137}\text{Cs}$  in single-crystalline SYNROC [17–23].

#### 4. Conclusions

In conclusion, single crystals of cesium titanate hollandite,  $\text{Cs}_{1.35}\text{Ti}_8\text{O}_{16}$ , were prepared electrochemically in a molten mixture of  $\text{Cs}_2\text{MoO}_4$  and  $\text{TiO}_2$ . The electrochemical preparation of  $\text{Cs}_{1.35}\text{Ti}_8\text{O}_{16}$  will be available for the practical disposal of the  $^{137}\text{Cs}$  contained in nuclear wastes because it enables the production of a SYNROC material that offers the following advantages: it requires moderate preparation conditions, is capable of immobilizing a high content of  $^{137}\text{Cs}$  ions in a highly stable form of single crystals.

#### Appendix A. Supplementary materials

Supplementary data associated with this article can be found in the online version at [doi:10.1016/j.jssc.2006.02.005](https://doi.org/10.1016/j.jssc.2006.02.005).

#### References

- [1] K.J. Nikula, B.A. Muggenburg, W.C. Griffith, W.W. Carlton, T.E. Fritz, B.B. Boecker, *Radiat. Res.* 146 (1996) 536–547.
- [2] A.E. Ringwood, S.E. Kesson, N.G. Ware, W. Hibberson, A. Major, *Nature* 278 (1979) 219–223.
- [3] S.E. Kesson, *Radioactive Waste Manage. Nucl. Fuel Cycle* 4 (1983) 53–72.
- [4] D.M. Levins, R.S.C. Smart, *Nature* 309 (1984) 776–778.
- [5] A.E. Ringwood, S.E. Kesson, D.M. Levins, E.J. Ramm, in: W. Lutze, R.C. Ewing (Eds.), *Radioactive Waste Forms for the Future*, Elsevier, Amsterdam, 1988, pp. 233–334.
- [6] H.U. Beyeler, C. Schüler, *Solid State Ionics* 1 (1980) 77–86.
- [7] S.E. Kesson, T.J. White, *Proc. R. Soc. London A* 405 (1986) 73–101.
- [8] M. Latroche, L. Brohan, R. Marchand, M. Tournoux, *Mater. Res. Bull.* 25 (1990) 139–148.
- [9] R.W. Cheary, *Acta Crystallogr. B* 47 (1991) 325–333.
- [10] A.F. Reid, J.A. Watts, *J. Solid State Chem.* 1 (1970) 310–318.
- [11] E. Fanchon, J.L. Hodeau, J. Vicat, J.A. Watts, *J. Solid State Chem.* 92 (1991) 88–100.
- [12] J. Ovenstone, K. Yanagisawa, *Chem. Mater.* 11 (1999) 2770–2774.
- [13] H. Abe, K. Nishida, M. Imai, H. Kitazawa, *J. Cryst. Growth* 267 (2004) 42–46.
- [14] W.H. McCarroll, K.V. Ramanujachary, M. Greenblatt, F. Cosandey, *J. Solid State Chem.* 136 (1998) 322–327.
- [15] W.H. McCarroll, Ian D. Fawcett, M. Greenblatt, K.V. Ramanujachary, *J. Solid State Chem.* 146 (1999) 88–95.
- [16] W.H. McCarroll, K.V. Ramanujachary, M. Greenblatt, *J. Solid State Chem.* 130 (1997) 327–329.
- [17] H. Xu, A. Navrotsky, M. Nyman, T.M. Nenoff, *J. Am. Ceram. Soc.* 88 (2005) 1819–1825.
- [18] L.M. Wang, J. Chen, R.C. Ewing, *Curr. Opin. Solid State Mater. Sci.* 8 (2004) 405–418.
- [19] H. Xu, A. Navrotsky, M.L. Balmer, Y. Su, *J. Am. Ceram. Soc.* 85 (2002) 1235–1242.
- [20] H. Xu, A. Navrotsky, M.L. Balmer, Y. Su, E.R. Bitten, *J. Am. Ceram. Soc.* 84 (2001) 555–560.
- [21] M.L. Balmer, Y. Su, H. Xu, E. Bitten, D. McCready, A. Navrotsky, *J. Am. Ceram. Soc.* 84 (2001) 153–160.
- [22] M. Nyman, F. Bonhomme, D.M. Teter, R.S. Maxwell, B.X. Gu, L.M. Wang, R.C. Ewing, T.M. Nenoff, *Chem. Mater.* 12 (2000) 3449–3458.
- [23] M.L. Balmer, Q. Huang, W. Wong-Ng, R.S. Roth, A. Santono, *J. Solid State Chem.* 130 (1997) 97–102.